Journal of Volcanology and Geothermal Research 306 (2015) 1–16

Contents lists available at ScienceDirect

Journal of Volcanology and Geothermal Research

journal homepage: www.elsevier.com/locate/jvolgeores

Contrasting records from mantle to surface of Holocene lavas of two nearby arc volcanic complexes: Caburgua-Huelemolle Small Eruptive Centers and Villarrica Volcano, Southern Chile

E. Morgado [a,*], M.A. Parada [a], C. Contreras [a], A. Castruccio [a], F. Gutiérrez [a,b], L.E. McGee [a]

[a] Departamento de Geología, Facultad de Ciencias Físicas y Matemáticas, Universidad de Chile, Chile/Centro de Excelencia en Geotermia de los Andes (CEGA), Chile
[b] Advanced Mining Technology Center, Universidad de Chile, Chile

ARTICLE INFO

Article history:
Received 4 April 2015
Accepted 24 September 2015
Available online 3 October 2015

Keywords:
Small eruptive centers
Villarrica Volcano
Reservoir depth
Reservoir heating

ABSTRACT

Most of the small eruptive centers of the Andean Southern Volcanic Zone are built over the Liquiñe-Ofqui Fault Zone (LOFZ), a NS strike-slip (>1000 km length) major structure, and close to large stratovolcanoes. This contribution compares textural features, compositional parameters, and pre- and syn-eruptive P,T conditions, between basaltic lavas of the Caburgua-Huelemolle Small Eruptive Centers (CHSEC) and the 1971 basaltic andesite lava of the Villarrica Volcano located 10 km south of the CHSEC. Olivines and clinopyroxenes occur as phenocrysts and forming crystal clots of the studied lavas. They do not markedly show compositional differences, except for the more scattered composition of the CHSEC clinopyroxenes. Plagioclase in CHSEC lavas mainly occur as phenocrysts or as microlites in a glass-free matrix. Two groups of plagioclase phenocrysts were identified in the 1971 Villarrica lava based on crystal size, disequilibrium features and zonation patterns. Most of the CHSEC samples exhibit higher La_N/Yb_N and more scattered Sr–Nd values than 1971 Villarrica lava samples, which are clustered at higher $^{143}Nd/^{144}Nd$ values. Pre-eruptive temperatures of the CHSEC-type reservoir between 1162 and 1165 ± 6 °C and pressures between 10.8 and 11.4 ± 1.7 kb consistent with a deep-seated reservoir were obtained from olivine–augite phenocrysts. Conversely, olivine–augite phenocrysts of 1971 Villarrica lava samples record pre-eruptive conditions of two stages or pauses in the magma ascent to the surface: 1208 ± 6 °C and 6.3–8.1 kb ± 1.7 kb (deep-seated reservoir) and 1164–1175 ± 6 °C and ≤1.4 kb (shallow reservoir). At shallow reservoir conditions a magma heating prior to the 1971 Villarrica eruption is recorded in plagioclase phenocrysts. Syn-eruptive temperatures of 1081–1133 ± 6 °C and 1123–1148 ± 6 °C were obtained in CHSEC and 1971 Villarrica lava, respectively using equilibrium olivine–augite microlite pairs. The LOFZ could facilitate a direct transport to the surface of the CHSEC magmas and explain the observed differences with the pre-eruptive conditions of the 1971 Villarrica lava.

1. Introduction

Small eruptive centers are present in different tectonic settings and are associated with products of different compositions, although they commonly are basaltic (Valentine and Gregg, 2008; Németh, 2010; McGee et al., 2011). For example, the Jeju Island Quaternary intraplate volcanic field in Korea, is composed of alkali and sub-alkali basaltic monogenetic centers clustered on a few kilometers scale (Park et al., 1999) that were derived from a heterogeneous mantle source and independent reservoirs (Brenna et al., 2012). In the western Mexican trans-arc, the Tequila volcanic field has a bimodal composition probably caused by the emplacement of basalts that trigger partial melting of upper crustal rocks (Lewis-Kenedi et al., 2005). Many field of small eruptive centers consist of aligned volcanic cones clustered along regional structures (e.g. Connor et al., 1992, 2000; López-Escobar et al., 1995a; Condit and Connor, 1996; Conway et al., 1998; Valentine and Perry, 2006) and they commonly were formed by short-lived multiple eruption phases (e.g. Houghton and Schmincke, 1989; Brand and White, 2007).

Many attempts to explain the reasons why small eruptive centers and polygenetic volcanism can co-exist have been focused on explanations considering structural aspects and magmatic rates. For example, crack interaction theory indicates that both high regional differential stress and low magma supply rate allow the development of small volcano fields because they prevent to generate crack coalescence, to from large polygenetic volcanoes (Takada, 1994). Conversely, Cañón-Tapia and Walker (2004) suggest that the most important controlling factor

* Corresponding author at: Centro de Excelencia de Geotermia de los Andes (CEGA), Departamento de Geología, Facultad de Ciencias Físicas y Matemáticas, Universidad de Chile, Santiago 8370450, Chile.

E-mail addresses: emorgado@ing.uchile.cl (E. Morgado), maparada@cec.uchile.cl (M.A. Parada), clcontre@ug.uchile.cl (C. Contreras), acastruc@ing.uchile.cl (A. Castruccio), frgutier@ing.uchile.cl (F. Gutiérrez), lucymcgee@ing.uchile.cl (L.E. McGee).

http://dx.doi.org/10.1016/j.jvolgeores.2015.09.023
0377-0273/

for the small eruptive center formation with respect to stratovolcanoes is the degree of melt interconnection through coalescing conduits where the magma ascends. On the other hand, Pinel and Jaupart (2000) proposed that for a given edifice dimension there is a critical magma density threshold over which the magma cannot reach the surface. The stalled magmas could evacuate by horizontally propagating dykes that feed small centers (Pinel and Jaupart, 2004).

Small eruptive centers of the Chilean Southern Andes are the most primitive volcanoes of the Southern Volcanic Zone (SVZ; Hildreth and Moorbath, 1988) and are commonly built over of the dextral strike-slip Liquiñe-Ofqui Fault Zone (LOFZ) and close to large stratovolcanoes (Gutiérrez et al., 2005; Lara et al., 2006a; Cembrano and Lara, 2009). Regional structural studies concluded that some Andean SECs are spatially associated with NE–SW tension fractures, along which a rapid magma ascent is facilitated (e.g. López-Escobar et al., 1995a; Lara et al., 2006a; Cembrano and Lara, 2009). Geochemical and isotopic studies allowed constraining the nature of the magma source (Hickey-Vargas et al., 1989; 2002) and indicated that Andean stratovolcanoes and SECs had similar asthenospheric sources, but different melting degrees (López-Escobar et al., 1995a) and ascent pathways (Lara et al., 2006a,2006b). They also concluded that differences between the Villarrica volcano and CHSEC could be explained by independent origins from

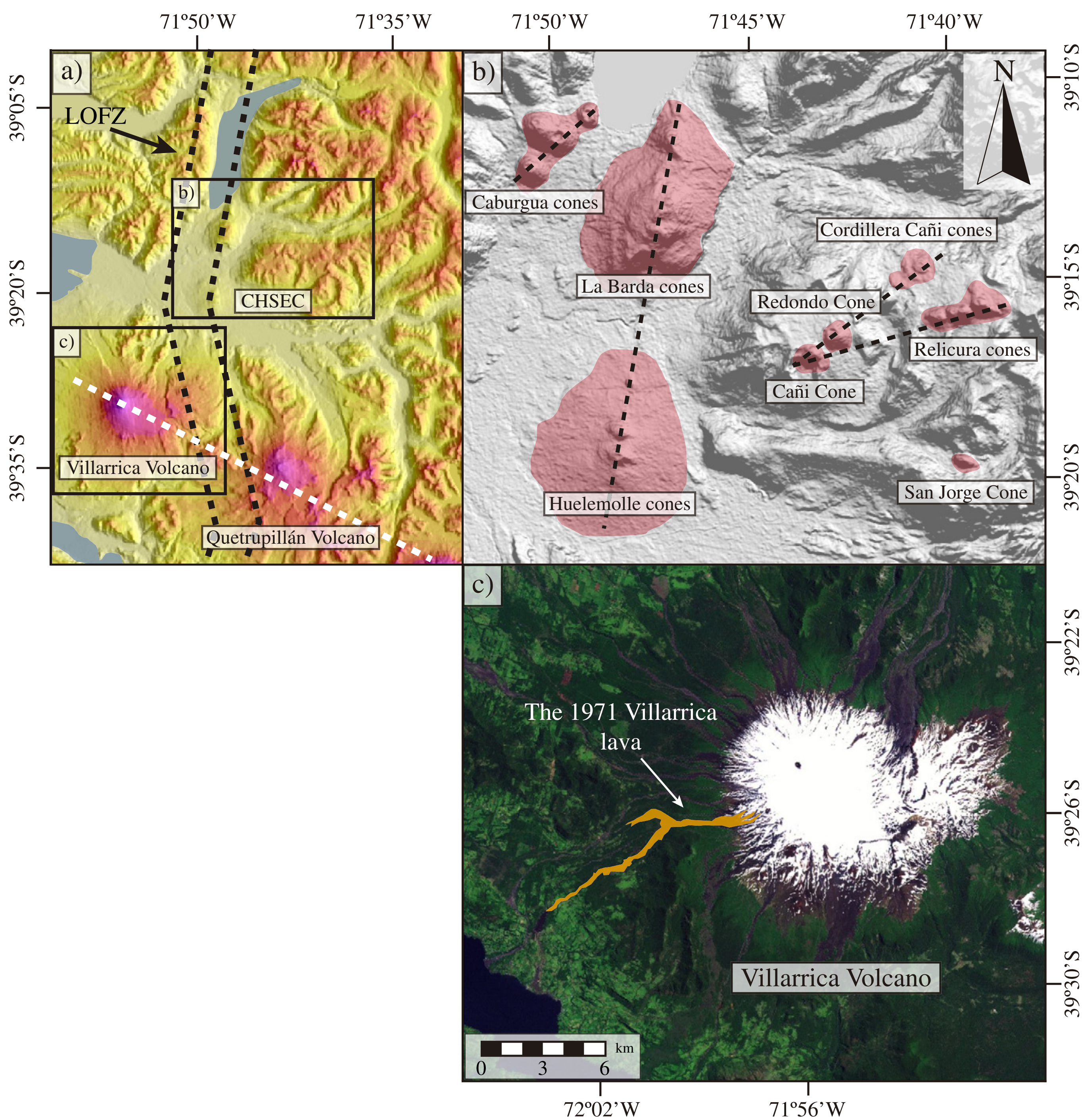

Fig. 1. a) Location of the Villarrica and Quetrupillán Stratovolcanoes and the Liquiñe Ofqui Fault Zone (LOFZ, black-dashed lines; Cembrano et al., 1996). The NW–SE volcanic chain that includes Villarrica, Quetrupillán and Lanín stratovolcanoes is represented by white-dashed line. b) Distribution of the CHSEC cones. Dashed lines represent cone alignments that coincide with the NNE-striking faults and NE-striking tension cracks (Cembrano and Lara, 2009) associated with LOFZ c) Villarrica Volcano and the lava erupted during the 1971 eruption.

heterogeneous sources, probably associated to variable effects of slab-derived fluids. Differences in major and trace elements and isotopic ratios have been observed between San Jorge cone and the rest of the CHSEC. However, San Jorge rocks are similar to those obtained in the Villarrica lavas, which let to suggest a geochemical connection between Villarrica volcano and at least one of the CHSEC (Hickey-Vargas et al., 2002).

The present study focuses on lavas of the Caburgua-Huelemolle Small Eruptive Centers (CHSEC) and the 1971 lava of the neighboring Villarrica Volcano of the SVZ. The latter lava was selected because it corresponds to a large and the best preserved Holocene lava of the Villarrica Volcano. CHSEC are composed of 21 pyroclastic cones with associated lava flows of basaltic composition that are assembled into 8 volcanic centers: Caburgua, Huelemolle, La Barda, Relicura, Cañi, Redondo, Cordillera Cañi and San Jorge (Fig. 1). Four lavas from cones of Caburgua, three lavas from each cone of Huelemolle, one lava sample from the San Jorge cone and 5 samples from the 1971 Villarrica lava were selected to study the pre-eruptive conditions from the magma reservoirs up to the surface using whole-rock geochemistry, mineral chemistry, and thermobarometric tools. Particular emphasis is placed on the existence of reservoirs at different depths in both volcanic complexes and deciphering the plumbing system to the surface of the respective magmas. We attempt to test the hypothesis that the Villarrica stratovolcano has an upper-crustal reservoir from which successive eruptions were supplied, whereas CHSEC magma directly rises from depth along the LOFZ.

1.1. Caburgua-Huelemolle Small Eruptive Centers (CHSEC)

CHSEC are located at the south of Caburgua Lake (Fig. 1), 10 km north of Villarrica Volcano. Some of the small eruptive centers correspond to volcanic cone clusters: Caburgua (five cones), Huelemolle (three cones), La Barda (three cones), Relicura (five cones), and Cordillera Cañi (two cones). Cañi, Redondo and San Jorge are volcanic centers formed by a single cone (Fig. 1). Two directions of cone alignments are recognized (Fig. 1): NNE that coincides with the dextral Liquiñe-Ofqui Fault (LOFZ) and NE that coincides with tension cracks (duplex) of the LOFZ (Cembrano et al., 1996; Cembrano and Lara, 2009). The main characteristics of CHSEC cones are provided in Table 1.

The CHSEC lavas are basalts (49–52 wt.%; Table 2) that contain plagioclase, olivine and clinopyroxene pheonocrysts with glomeroporphiric, traquitic and intergranular textures. Most of the CHSEC lavas are phenocryst-poor (3–10 vol.%), with the exception of the San Jorge lava, which has phenocryst content of 13–18 vol.%. The percentage of vesicles in CHSEC varies between 4 and 14 vol.%.

The age of the Huelemolle volcanic activity was estimated as at least 9000 years old by a ^{14}C dating of carbonized wood collected into pyroclastic deposits (Moreno and Clavero, 2006; Moreno and Lara, 2008). The ages for the other small eruptive centers are not well-constrained but the absence of glacial erosion suggests being post-glacial Holocene.

1.2. Summary of Villarrica Volcano and its 1971 eruption

Villarrica Volcano is one of the most active volcanic centers of the Southern Andean Volcanic Zone. Its height is 2828 m.a.s.l., with an estimated volume of 250 km^3 that covers an area of 400 km^2. It is located at the westernmost position of the NW–SE volcanic chain that also includes Quetrupillán and Lanín stratovolcanoes (López-Escobar et al., 1995b; Stern et al., 2007). Villarrica Volcano, which started its activity at least 600 ky ago (Moreno and Clavero, 2006) and has produced basalts and basaltic andesite lava flows and pyroclastic deposits, which are divided into three units (Clavero and Moreno, 2004; Moreno and Clavero, 2006): Villarrica I (Middle to Upper Pleistocene), Villarrica II (Holocene, between 13.9 and 3.7 ky) and Villarrica III (<3.7 ky). Unit Villarrica III has a historical record of eruptions; some of them correspond to lavas of the following eruptions: 1787, 1921, 1948, 1963, 1964, 1971 and 1984. Two major explosive events of mafic to intermediate composition have been significant in the Holocene development of Villarrica Volcano: the ~13 ky Licán Ignimbrite (~10 km^3, non-Dense Rock Equivalent; Clavero and Moreno, 1994; Lohmar et al., 2007) and the ~3.5 ky Pucón Ignimbrite (~3 km^3, non-Dense Rock Equivalent; Clavero and Moreno, 1994; Silva et al., 2004).

Currently, the volcano is characterized by a lava lake and constant degassing and seismicity (Calder et al., 2004). The 1971 Villarrica eruption generated two Aa-type lavas. The eruption began in October with strombolian explosions and lava effusions along the Challupén Valley (SW flank). In November, two pyroclastic cones grew inside the crater simultaneously with lava effusion. During the night of the December 30th, the eruption reached its paroxysmal phase, with a lava fountain > 500 m high and effusion rates ~ 500m^3/s, generating two lava flows of 6 and 16.5 km that flowed along the Pedregoso and Challupén valleys, respectively and were emplaced in less than 48 h. The total erupted volume is ~ 0.03 km^3 (Moreno, 1993; Moreno and Clavero, 2006 and references therein). The studied lava has phenocrysts (14–17 vol.%) of plagioclase, olivine and clinopyroxenes, and vesicles that reach up to 13 vol.%. The most common textures are glomeroporphiric, traquitic, poikilitic, ophitic and subophitic.

2. Analytical procedure

Sixteen samples from CHSEC lavas and five from the 1971 Villarrica lava were studied for geochemical, isotopic and mineralogical analysis. The CHSEC samples were collected from three *Pahoehoe* lavas of Caburgua, three Aa lavas of Huelemolle, and one of each *Aa* lava of San Jorge, La Barda, Relicura, Cañi, Redondo and Cordillera Cañi. Five samples were collected along the 1971 Villarrica lava. Whole-rock compositions were analyzed by XRF (major elements) and ICP-MS (trace elements) at ACT-Labs using BIR-1a, DNC-1, W-2a and DNC-1 standards. The precision was <9% 2σ and accuracy was mostly better than 3%. The Sr and Nd isotope data were obtained for 8 samples (one sample for each CHSEC) with a Triton multi-collector mass-spectrometer at ACT-Labs using the standards JNd-1 (for Nd isotopes) and NBS 987

Table 1
Main features of CHSEC (cones of each SEC were ordened from north to south).

Eruptive center/cone	Max. height (m.a.s.l.)	Cone height (m)	Cone volume[a] (km^3)	Alignment (of the SEC)
Caburgua SEC				N50E
Caburgua 1	680	152	0.033	
Caburgua 2	751	244	0.104	
Caburgua 3	980	414	0.308	
Caburgua 4	755	331	0.135	
Caburgua 5	490	380	–	
Huelemolle SEC				N15E
Huelemolle 1	560	102	0.013	
Huelemolle 2	820	450	1.91	
Huelemolle 3	859	489	2.076	
La Barda SEC				N10E
La Barda 1	678	271	0.054	
La Barda 2	941	444	0.203	
La Barda 3	1209	696	4.69	
Relicura SEC				N70E
Relicura 1	1537	98	0.002	
Relicura 2	1648	287	0.011	
Relicura 3	1571	263	0.005	
Relicura 4	1598	290	0.005	
Relicura 5	1507	176	0.003	
Cordillera Cañi				N45E
Cordillera Cañi 1	1302	69	0.0004	
Cordillera Cañi 1	1324	91	0.0009	
Other SECs				
Cañi cone	1462	152	0.004	
Redondo cone	1483	153	0.006	
San Jorge cone	1120	150	0.004	

[a] The procedures for volume estimation were identical to those described by Aravena and Lahsen (2012).

Table 2
Whole rock analyses of samples from CHSEC and the 1971 Villarrica eruption. Only Caburgua, San Jorge, and Huelemolle data were used in diagrams (Figs. 2 and 3). All available isotopic data were used in Fig. 4.

	Caburgua					
	Detection limit	Cab1-1	Cab1-2	Cab2-1	Cab2-2	Cab3-1
SiO2	0.01 (%)	50.26	49.88	50.24	51.31	50.78
Al2O3	0.01 (%)	17.48	17.5	17.5	17.45	17.56
TiO2	0.001 (%)	1.116	1.108	1.144	1.13	1.14
FeO	0.1 (%)	6.6	5.7	7.2	5.8	7.4
Fe2O3	0.01 (%)	2.97	3.72	2.45	4.33	2.38
MnO	0.001 (%)	0.149	0.149	0.15	0.156	0.154
MgO	0.01 (%)	6.8	6.71	6.33	7.45	7.06
CaO	0.01 (%)	8.68	8.92	8.79	8.84	8.72
Na2O	0.01 (%)	3.3	3.22	3.34	3.33	3.37
K2O	0.01 (%)	0.75	0.68	0.82	0.75	0.8
P2O5	0.01 (%)	0.29	0.31	0.34	0.33	0.34
LOI		−0.09	0.09	−0.34	0.03	−0.22
Rb	2 (ppm)	10	9	12	9	11
Sr	2 (ppm)	798	779	753	773	773
Zr	4 (ppm)	79	81	92	85	89
Y	2 (ppm)	17	18	17	18	18
Nb	1 (ppm)	5	5	6	4	5
Ta	0.1 (ppm)	0.2	0.2	0.2	0.5	0.5
Ba	3 (ppm)	266	263	285	270	280
U	0.1 (ppm)	0.7	0.7	0.7	0.6	0.7
Th	0.1 (ppm)	2.7	2.7	3.3	2.5	2.7
Pb	5 (ppm)	7	7	8	10	8
La	0.1 (ppm)	14.4	16.3	17.7	14.4	17.6
Ce	0.1 (ppm)	31.5	35.1	39	31.7	37.1
Pr	0.05 (ppm)	4.14	4.65	5.03	4.24	4.71
Nd	0.1 (ppm)	17.6	19.3	21	18	20
Sm	0.1 (ppm)	3.9	4.3	4.6	4	4.4
Eu	0.05 (ppm)	1.2	1.25	1.41	1.26	1.3
Gd	0.1 (ppm)	3.8	3.9	4.3	4	3.9
Tb	0.1 (ppm)	0.6	0.6	0.7	0.6	0.6
Dy	0.1 (ppm)	3.2	3.5	3.7	3.4	3.4
Ho	0.1 (ppm)	0.6	0.7	0.7	0.7	0.7
Er	0.1 (ppm)	1.8	2	2	1.9	2
Tm	0.05 (ppm)	0.26	0.28	0.29	0.26	0.29
Yb	0.1 (ppm)	1.7	1.9	1.9	1.7	1.9
Lu	0.04 (ppm)	0.28	0.32	0.31	0.28	0.33
$^{87}Sr/^{86}Sr$			0.703762 ± 4			
$^{143}Nd/^{144}Nd$			0.512849 ± 2			

	San Jorge		Huelemolle			
	Sanj-1	Sanj-3	Huel-1	Huel-3	Huel-4	Huel-6
SiO2	50.29	49.37	49.96	50.95	51.77	50.12
Al2O3	15.63	15.51	17.73	18.22	17.76	18.19
TiO2	0.804	0.763	1.106	1.129	1.194	1.139
FeO	6.3	7.7	7.7	6.6	7.3	6
Fe2O3	3.57	2.23	2.18	3.53	2.88	3.74
MnO	0.157	0.155	0.156	0.161	0.159	0.153
MgO	9.83	10.8	5.66	5.67	4.6	4.74
CaO	9.88	9.57	9.4	9.55	8.91	9
Na2O	2.5	2.46	3.17	3.23	3.56	3.33
K2O	0.41	0.41	0.82	0.83	0.93	0.83
P2O5	0.13	0.1	0.41	0.4	0.43	0.43
LOI	−0.12	−0.44	−0.16	−0.09	−0.23	0.44
Rb	7	7	13	13	14	13
Sr	375	361	593	613	627	633
Zr	54	46	132	137	143	136
Y	14	13	21	21	21	20
Nb	<1	<1	7	7	7	7
Ta	<0.1	0.8	0.4	0.3	0.4	0.3
Ba	140	132	305	315	343	314
U	0.2	0.2	0.6	0.6	0.6	0.6
Th	0.7	1.1	2	2.8	2.2	2.2
Pb	<5	5	9	10	10	10
La	6	6.5	22.7	23.1	23.1	22.6
Ce	13.5	14.6	48.1	49.3	49.7	47.9
Pr	1.8	2.04	5.87	6.13	6.03	5.92
Nd	8.3	8.9	24	24.9	24.5	23.6
Sm	2.1	2.2	5.1	5.2	5.2	5
Eu	0.75	0.77	1.49	1.49	1.53	1.45
Gd	2.6	2.6	4.7	4.6	4.9	4.7
Tb	0.4	0.4	0.7	0.7	0.7	0.7
Dy	2.5	2.4	4.2	4	4.1	4

Table 2 (*continued*)

	San Jorge		Huelemolle			
	Sanj-1	Sanj-3	Huel-1	Huel-3	Huel-4	Huel-6
Ho	0.5	0.5	0.8	0.8	0.8	0.8
Er	1.5	1.5	2.5	2.3	2.5	2.4
Tm	0.23	0.23	0.36	0.34	0.36	0.35
Yb	1.5	1.5	2.3	2.2	2.4	2.2
Lu	0.25	0.25	0.36	0.37	0.37	0.35
$^{87}Sr/^{86}Sr$		0.703935 ± 4	0.703935 ± 4			
$^{143}Nd/^{144}Nd$		0.512848 ± 2	0.512848 ± 2			

	Other SECs				
	Barda1-2	Rel1-2	Cañi-5	Red-5	Cord2-2
SiO2	50.45	51.22	50.49	50.87	49.85
Al2O3	16.82	17.55	17.32	17.24	17.28
TiO2	1.077	1.167	1.023	0.994	1.165
FeO	6.9	8.4	7.3	7.9	4.8
Fe2O3	3.09	2.61	2.61	2.01	4.72
MnO	0.154	0.163	0.148	0.153	0.152
MgO	7.59	5.79	6.65	7.35	6.42
CaO	9.07	8.46	8.45	9.07	8.19
Na2O	3.13	3.29	3.17	3.08	3.28
K2O	0.74	1.11	0.85	0.79	1.23
P2O5	0.33	0.41	0.32	0.29	0.44
LOI	−0.08	−0.33	−0.18	−0.23	0.5
Rb	10	21	14	13	24
Sr	672	614	582	13	652
Zr	91	154	118	106	157
Y	18	21	18	18	21
Nb	3	6	4	4	10
Ta	0.1	0.4	0.2	0.3	0.6
Ba	260	397	305	280	440
U	0.6	0.8	0.5	0.5	0.9
Th	2.2	3.3	1.8	2	3.3
Pb	7	9	8	7	9
La	15	24.4	17.7	17.1	26.4
Ce	33	50.8	37	35.8	54.1
Pr	4.33	6.13	4.59	4.46	6.58
Nd	18.2	25.3	18.4	18.1	26.6
Sm	4	5.3	4.1	4.1	5.4
Eu	1.18	1.48	1.21	1.17	1.62
Gd	3.5	4.8	3.8	3.7	4.9
Tb	0.6	0.7	0.6	0.6	0.7
Dy	3.2	4.2	3.3	3.3	4.1
Ho	0.6	0.8	0.6	0.7	0.8
Er	1.9	2.4	1.8	1.9	2.3
Tm	0.27	0.34	0.27	0.28	0.35
Yb	1.7	2.1	1.7	1.8	2.2
Lu	0.28	0.34	0.27	0.29	0.34
$^{87}Sr/^{86}Sr$	0.703837 ± 4	0.704005 ± 4	0.703978 ± 4	0.703963 ± 4	0.703973 ± 4
$^{143}Nd/^{144}Nd$	0.512873 ± 2	0.512814 ± 2	0.512913 ± 2	0.512821 ± 2	0.512801 ± 2

	1971 Villarrica lava				
	1971 N6	1971 10 M1	1971 09	1971 30	R1971 DV
SiO2	52.85	51.92	52.47	52.93	51.76
Al2O3	16.76	16.68	16.71	16.77	16.59
TiO2	1.105	1.117	1.113	1.132	1.13
FeO	7.2	6.6	6.7	7.1	5.5
Fe2O3	3.05	3.17	3.31	2.83	4.55
MnO	0.157	0.154	0.154	0.154	0.154
MgO	6.39	5.95	6.1	6.02	6.1
CaO	9.76	9.57	9.61	9.63	9.55
Na2O	3.06	3.01	3.06	3.08	2.98
K2O	0.64	0.64	0.65	0.65	0.63
P2O5	0.21	0.23	0.23	0.18	0.2
LOI	−0.61	−0.47	−0.51	−0.55	−0.41
Rb	14	14	15	15	14
Sr	414	420	420	428	417
Zr	85	86	87	87	85
Y	22	22	22	22	21
Nb	1	1	1	2	1
Ta	<0.1	<0.1	0.1	<0.1	<0.1
Ba	201	199	200	198	197
U	0.4	0.4	0.4	0.5	0.4

(continued on next page)

Table 2 (*continued*)

	1971 Villarrica lava				
	1971 N6	1971 10 M1	1971 09	1971 30	R1971 DV
Th	1.2	1.2	1.2	1.3	1.2
Pb	6	7	7	8	6
La	6.9	7.2	7.3	8	7
Ce	17.5	17.8	17.8	19.7	17.3
Pr	2.56	2.67	2.64	2.72	2.62
Nd	12	12.3	12.5	13.3	12.5
Sm	3.4	3.5	3.6	3.6	3.2
Eu	0.97	0.99	1.02	1.03	0.93
Gd	3.6	3.7	3.9	3.7	3.5
Tb	0.6	0.6	0.7	0.7	0.6
Dy	3.7	3.8	3.8	3.9	3.6
Ho	0.8	0.8	0.8	0.8	0.8
Er	2.3	2.3	2.3	2.3	2.4
Tm	0.37	0.36	0.35	0.35	0.37
Yb	2.4	2.3	2.3	2.2	2.3
Lu	0.34	0.33	0.35	0.35	0.32
$^{87}Sr/^{86}Sr$					
$^{143}Nd/^{144}Nd$					

(for Sr isotopes). The mineralogical studies were carried out with a Scanning Electron Microscope (SEM) at the University of Chile (FEI Quanta 250) and electron microprobe at the School of Geosciences, University of Edinburgh (Cameca SX100; nine samples) and at LAMARX-National University of Cordoba (JEOL JXA-8230; six samples). The analytical conditions for the eight CHSEC samples analyzed by the Cameca SX100 consisted of an accelerating potential of 15 kV and electron beam current of 4 nA for major elements and 100 nA for minor and trace elements. Counting times for major elements were 20 s on peak and 10 s on background. The mineral composition of the two samples from CHSEC and four from 1971 Villarrica lava measured by the JEOL JXA 8230 were obtained with an accelerating potential of 15 kV and electron beam current of 20 nA (10 nA for plagioclase). Counting times were 10 s for peak and 5 s at each background position for major and minor elements.

3. Geochemical and isotopic data

The analyzed CHSEC lavas are basalts (49.37–51.77%) and have lower SiO_2 contents than the 1971 Villarrica basaltic–andesite samples (51.76–52.93%) (Fig. 2a). All the CHSEC and Villarrica samples correspond to the calcalkaline series, except for San Jorge samples, which have tholeiitic affinities (Fig. 2b). The CHSEC have Mg# values between 0.48 and 0.69, whereas 1971 Villarrica samples have Mg# values between 0.56 and 0.59. For a given MgO composition, the CHSEC basalts have higher Al_2O_3, K_2O and P_2O_5 and lower Ni, Cr, Sc, V contents than Villarrica samples (Hickey-Vargas et al., 1989). Most CHSEC samples have similar trace element contents (Fig. 3) and La_N/Yb_N (5.94–8.34). The exceptions are the San Jorge samples, which have lower trace element contents and La_N/Yb_N (2.87–3.11). Villarrica rocks display La_N/Yb_N ratios between 2.06 and 2.67. All the samples display negative Nb–Ta (with the exception of the sample SANJ-3 that only shows negative Nb anomaly), Ti and Zr anomalies and positive Pb anomaly (Fig. 3a). CHSEC and Villarrica samples have small negative Eu anomalies (Fig. 3b). Most CHSEC samples have Dy_N/Yb_N (cf. Davidson et al., 2013) values between 1.07 and 1.34, similar to those values of the 1971 Villarrica lava samples (1.03 and 1.18).

Available and new data of Sr and Nd ratios of CHSEC and Villarrica are listed in Table 3 and plotted in Fig. 4. CHSEC samples have $^{87}Sr/^{86}Sr$ ratios in the range from 0.703762 ± 4 (Caburgua) to 0.704028 (San Jorge), whereas the $^{87}Sr/^{86}Sr$ ratios of the Villarrica samples are higher but within a narrower range from 0.70398 ± 3 (Unit Villarrica III) to 0.70410 ± 3 (Unit Villarrica I) (Hickey-Vargas et al., 1989). $^{143}Nd/^{144}Nd$ ratios of the CHSEC samples range from 0.512801 ± 2 (C. Cañi) to 0.512913 ± 4 (San Jorge), the Villarrica samples range from 0.512866 ± 22 (Unit Villarrica I) to 0.512903 ± 3 (Unit Villarrica III) (Hickey-Vargas et al., 1989). San Jorge and Cañi cones have

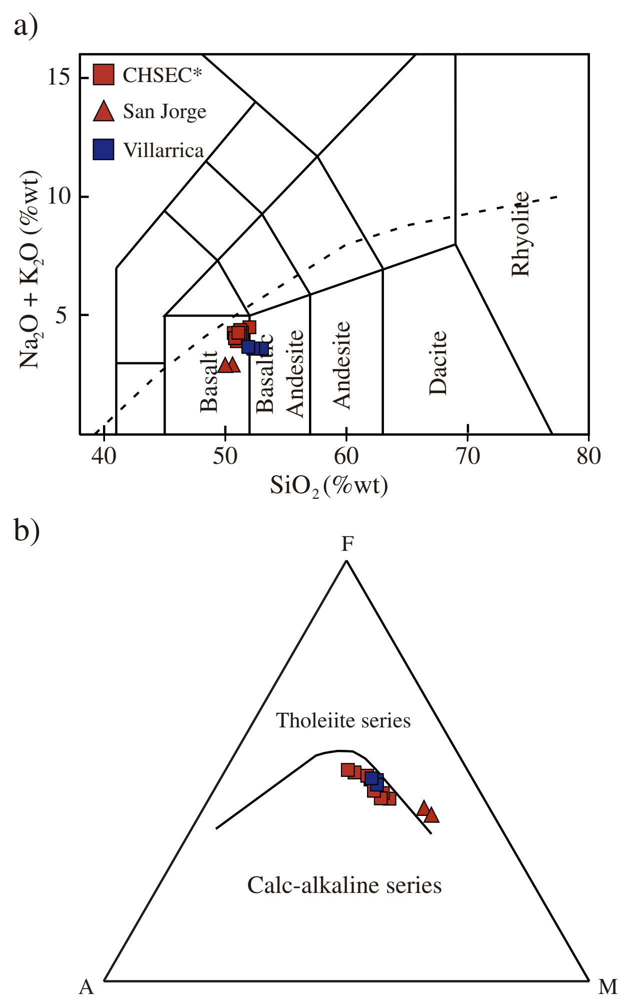

Fig. 2. a) Total alkali vs. silica (Le Bas et al., 1986) plots of CHSEC basalts and the 1971 Villarrica basaltic andesite lavas. Boundary dashed-line between alkaline and subalkaline rocks is taken from Irvine and Baragar (1971); b) AFM diagram (Irvine and Baragar, 1971) showing calc-alkaline trend for most of the CHSEC and the 1971 Villarrica lava samples. Lavas of San Jorge cone exhibit tholeiitic affinities.

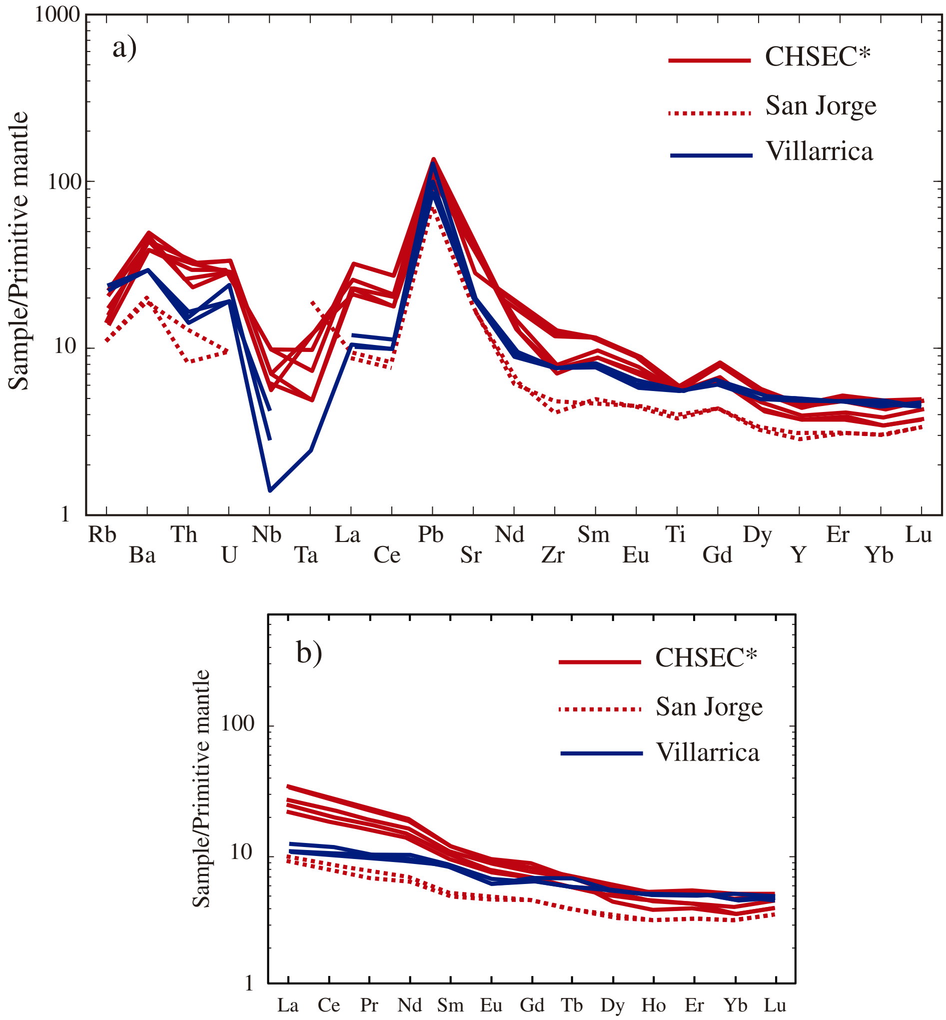

Fig. 3. Primitive mantle-normalized (Sun and McDonough, 1989) spider diagram (a) and REE patterns (b) of samples from the small eruptive centers and the 1971 Villarrica lava. CHSEC* includes all samples taken from the small eruptive centers, except those form San Jorge cone. Trace element concentrations lower than detection limit were omitted (see Table 2).

similar Sr–Nd isotopic values to those of Villarrica volcano and differ from those of the remainder CHSEC samples (Fig. 4).

4. Mineral chemistry

4.1. CHSEC plagioclases

Plagioclase phenocrysts are 0.7–2.0 mm in size and some of them have disequilibrium features in the form of patch and sieve textures. Plagioclase crystals of similar size also occur as clots with olivine, but unlike phenocrysts they do not exhibit disequilibrium features. The core compositions of plagioclase phenocrysts are fairly constant of An_{73-80} (Fig. 5a) and are similar in composition to the core plagioclase-forming clots. A thin rim (<40 μm) An_{45-65} is commonly found in plagioclase phenocrysts as well as in plagioclase-forming clots, but in the latter case only around crystal faces in contact with the matrix. CHSEC lavas have glass-free matrices with abundant microlites commonly forming part of a traquitic or intergranular

Table 3
Pressure and temperatures obtained from clots of crystals, oikocryst–chadacryst and microlites.

Eruptive center		T (±6 °C; Loucks, 1996)	P (±1.7 kb; Köhler and Brey, 1990)	Depth (km)
Villarrica	Clot of crystals	1208	6.3–8.1	19–35
	Oikocryst–chadacryst	1164–1175	0–0.7	0–9.8
	Microlites	1123–1148	–	
CHSEC	Phenocrysts (in contact)	1162–1165	10.8–11.4	32–44
	Microlites	1081–1133	–	

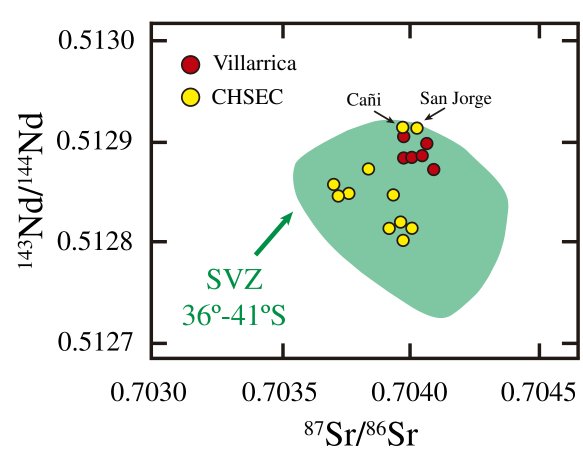

Fig. 4. $^{143}Nd/^{144}Nd$ versus $^{87}Sr/^{86}Sr$ plots, for CHSEC and Villarrica Volcano samples. Field of SVZ between 37 and 41°S are shown for comparison (data from López-Escobar et al., 1995a, 1995b and references therein). Data of Villarrica and CHSEC samples obtained by Hickey-Vargas et al. (1989) are included.

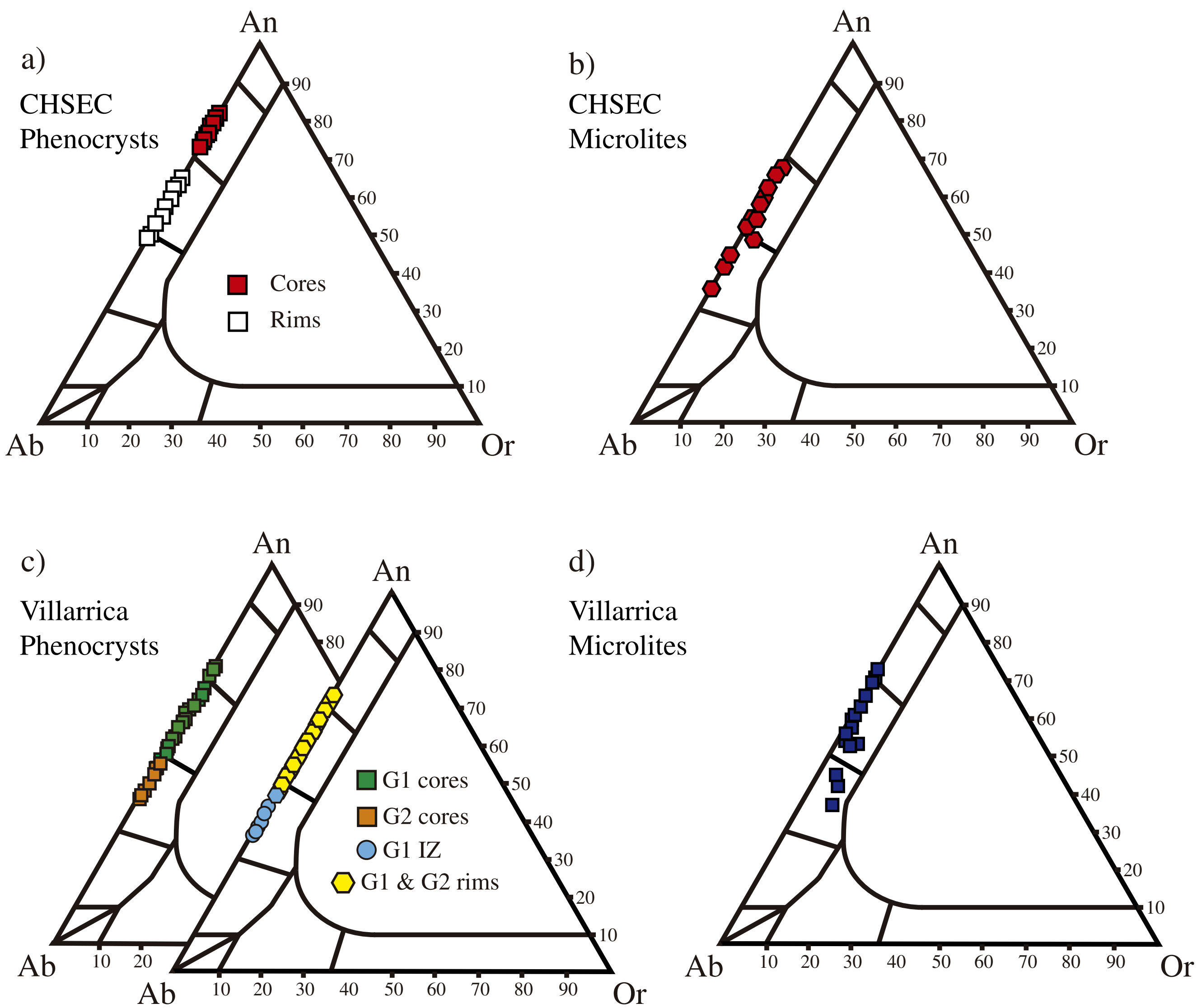

Fig. 5. Plagioclase compositions of the studied CHSEC and 1971 Villarrica lava samples. G.1, G.2: Group 1 and Group 2 plagioclase phenocrysts; IZ: intermediate zone of phenocrysts.

textures. The plagioclase microlite compositions are An_{45-58} (Fig. 5b). Some plagioclase microlites are hosted in plagioclase phenocryst rims indicating that, at least a portion of those rims grew coevally with microlites.

4.2. CHSEC mafic minerals and spinels

In CHSEC samples the olivine phenocrysts occur as isolated crystals or forming part of crystal clots together with plagioclase and commonly show disequilibrium features such as resorption and thin compositional rims. The core compositions of olivine phenocrysts and olivine-forming clots vary between Fo_{81} and Fo_{87} (Fig. 6a), and exhibit thin rims with compositions that vary between Fo_{73} and Fo_{80}. As with the plagioclase-forming clots, olivine-forming clots show rims only around non-armored faces. The olivine microlites occur as intergranular grains of 40–100 μm size with compositions in the Fo_{59-77} range (Fig. 6b). Clinopyroxene phenocrysts are very scarce and have compositions in the range of Wo_{44-46}, En_{45-47}, and Fs_{7-9} (Fig. 6c). Clinopyroxene microlites occur as small crystals of 5 and 92 μm and exhibit compositions in the range of Wo_{8-40}, En_{37-63}, and Fs_{13-31} (Fig. 6d).

Chromian-spinel inclusions are abundant in olivine phenocrysts and very scarce in plagioclase phenocrysts. They also occur as isolated crystals of 5–65 μm size or forming crystal clots. The composition of chromian-spinel inclusions are: #Cr = 25–39 and #Mg = 33–59. Titanomagnetites (Mt_{35-42}, Usp_{58-65}) were found as euhedral crystals or with skeletal features in the studied CHSEC samples except in San Jorge samples, where hematites were found. The size of the Fe–Ti oxide minerals vary between 5 and 30 μm.

4.3. 1971 Villarrica lava plagioclases

The modal content of plagioclase phenocrysts represents ~12% of the total rock volume (~60–80 vol.% of phenocrysts). Two groups of plagioclase phenocrysts were identified (Fig. 5c) according to crystal size and disequilibrium features. Group 1 includes 0.4–4.1 mm long phenocrysts with three zones (Fig. 7a): oscillatory-zoned core (An_{45-74}) normal-zoned intermediate zone (An_{38-44}) and reverse-zoned rim (An_{74-46}). The first two zones exhibit disequilibrium features in the form of patch and sieve textures. Group 2 (Fig. 7b) includes the smallest plagioclase phenocrysts (0.3–2.0 mm) that exhibit oscillatory-zoned cores of An_{39-49}, and thin reverse-zoned rims of An_{50-73}. These rim

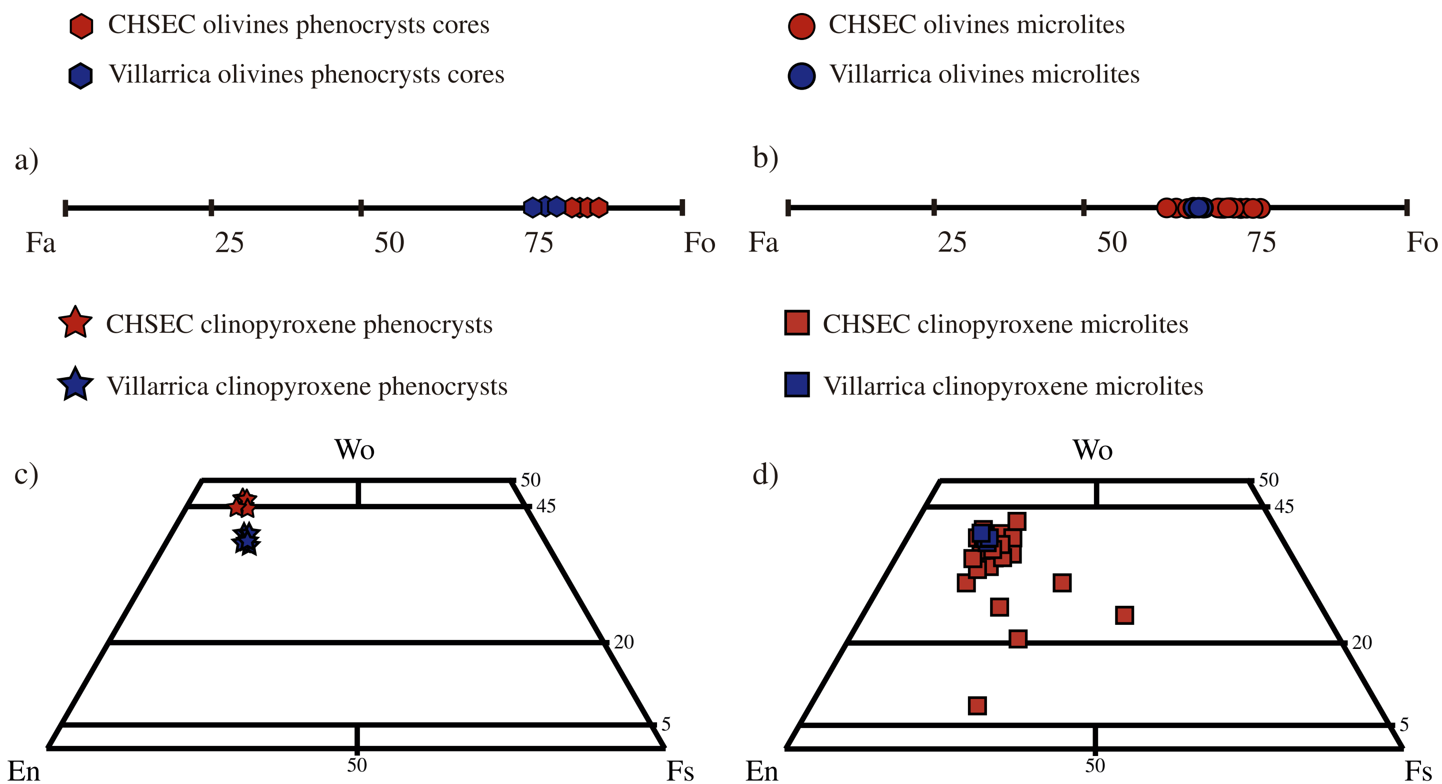

Fig. 6. Olivine and clinopyroxene compositions of the studied samples. Compositions of olivine phenocrysts (a) and microlites (b) of CHSEC and 1971 Villarrica lava. Compositions of clinopyroxene phenocrysts (c) and microlites (d) of the CHSEC and 1971 Villarrica lava.

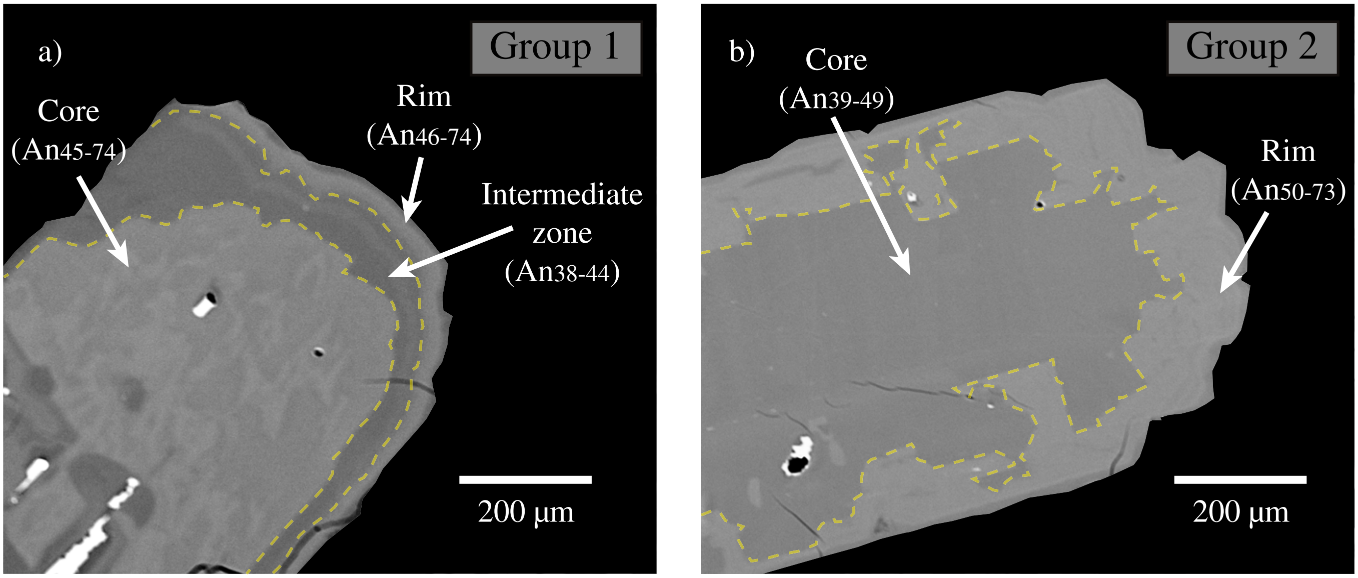

Fig. 7. a) Core, intermediate, and rim zones from Group 1 plagioclase phenocryst. Disequilibrium features are recognized in core zone. b) Core and rim zones from Group 2 plagioclase phenocryst. Disequilibrium features are recognized in core zone.

compositions are similar to the rim compositions of the Group 1 plagioclase phenocrysts (Fig. 5c). Large plagioclase crystals also occur as part of clots with olivine and scarce clinopyroxene and have compositions and sizes ($An_{51–73}$, 0.4–4.1 mm long) similar to the core of Group 1 plagioclases. Microlites of 1971 Villarrica samples (<300 μm) occupy ~85 vol.% of the glass free matrix and exhibit compositions of $An_{48–75}$ (Fig. 5b).

4.4. 1971 Villarrica lava mafic minerals and spinels

The modal content of the olivine phenocryst is between 2 and 4% and are found as isolated crystals (up to 4 mm long), forming clots (up to 4 mm long) or chadacrysts (~180 μm long). They have commonly resorption features and compositional rims that do not exceed 30 μm. The core compositions vary between Fo_{75} and Fo_{79} (Fig. 6a), and the rim composition slightly varies between Fo_{65} and Fo_{67}. The rims of olivine-forming clots are only developed around non-armored faces. The scarce olivine microlites (~5% of the groundmass) have sizes between 10 and 30 μm and compositions of $Fo_{63–67}$ (Fig. 6b) similar to the rim phenocryst composition. Clinopyroxenes of variable composition ($Wo_{37–40}$, $En_{47–49}$, Fs $_{12–13}$; Fig. 6c) occur as isolated crystals (0.6–1.5 mm) and oikocrysts within plagioclase and olivine chadacrysts. Clinopyroxene in the matrix varies between 15 and 40 μm long with compositions of $Wo_{8–17}$, $En_{57–65}$, and $Fs_{25–31}$ (Fig. 6d).

Chromian-spinel are found as inclusions of 15–50 μm in olivine phenocrysts and have compositions of #Cr = 53–62 and #Mg = 26–30. Titanomagnetite crystals of 5–20 μm and compositions of ($Mt_{33–44}$, $Usp_{56–67}$) were found as euhedral isolated crystals or exhibiting skeletal features in the matrix.

5. Results and discussion

5.1. Implications of the compositional signatures of the studied lavas

All the studied samples exhibit similar arc-related geochemical signatures such as calc-alkaline affinities (Fig. 2b) and negative Nb–Ta

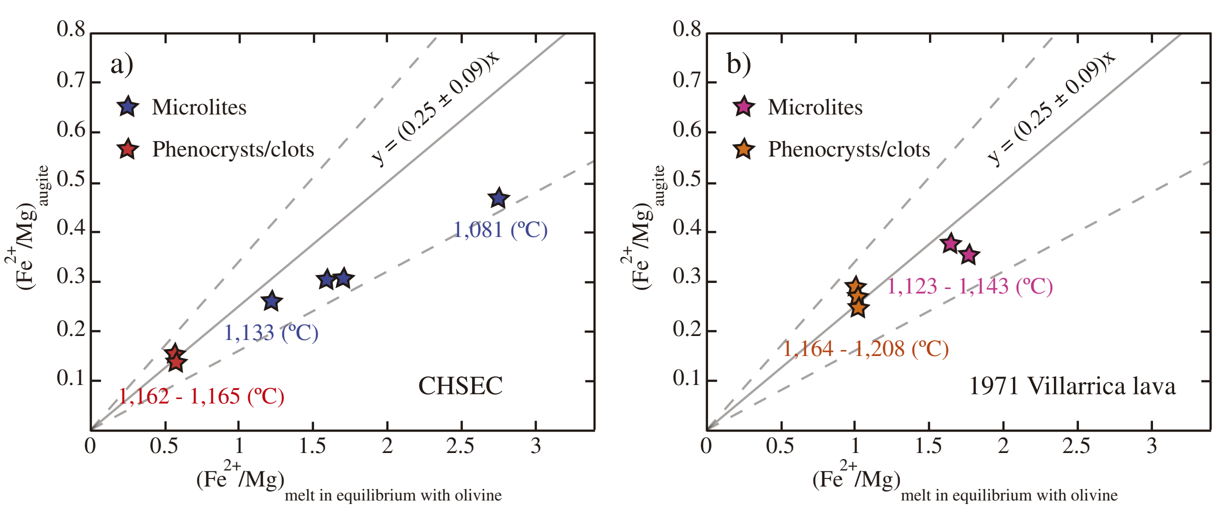

Fig. 8. Augite–melt equilibrium compositions for CHSEC (a) and the 1971 Villarrica lava (b) inferred from plot of $(Fe^{2+}/Mg)_{augite}$ versus $(Fe^{2+}/Mg)_{melt\ in\ equilibrium\ with\ olivine}$ and the $^{cpx\text{-}liq}K_D(Fe^{2+}/Mg)$ for clinopyroxene in equilibrium with H_2O-saturated basic melt (continuous lines) and associated errors (dashed lines), following Grove's et al., (1997) equation. Temperatures obtained for olivine–augite equilibrium (Loucks, 1996) are shown.

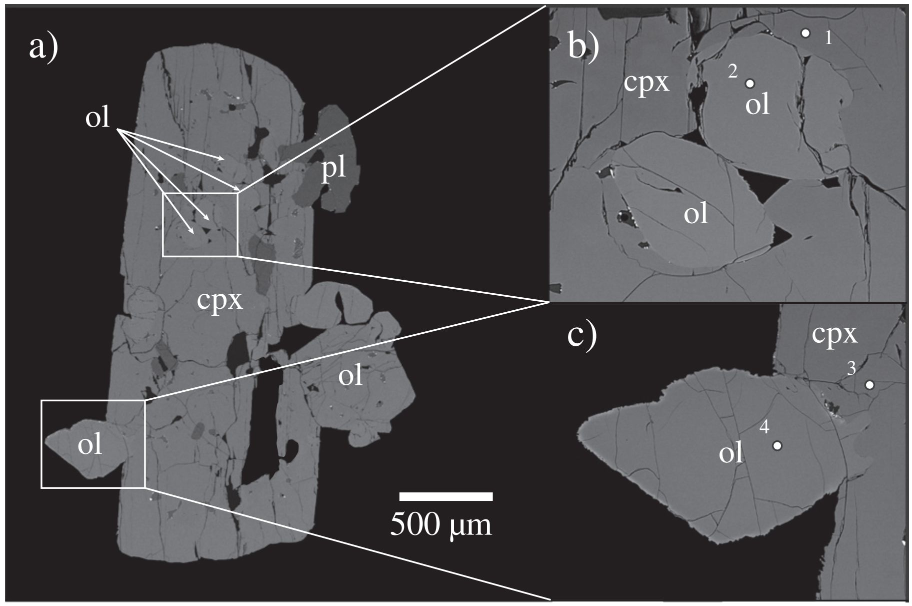

Fig. 9. a) Crystal clot of plagioclase, olivine and clinopyroxene. b) Details of olivine chadacrysts that gave equilibrium temperatures with the neighboring clinopyroxene of 1164 and 1175 ± 6 °C. c) Details showing thin rim in non-armored faces of the olivine. The equilibrium temperature of the olivine core–clinopyroxene is 1208 ± 6 °C. Numbered spots indicate the sites of EPM analyses. Analyses 1 (VI-pxph4), 2 (VI-olph4), 3 (VI-pxph5), and 4 (VI-olph5) are shown in Table 4.

anomalies (Fig. 3a). The presence of a slight negative Eu-anomaly in CHSEC and the 1971 Villarrica REE patterns suggest plagioclase as a residual phase in the studied lavas (Fig. 3b). Additionally, the wide range of Sr–Nd isotope ratios observed in CHSEC (Fig. 4), despite the proximity between centers, could indicate local-scale mantle source heterogeneities. The mantle is known to be heterogeneous beneath the SVZ (Jacques et al., 2013); many reasons have been suggested to explain these heterogeneities in detail related to other external factors such as the supply of terrigenous sediments (Stern, 1991, 2011; Kay et al., 2005), altered oceanic crust and upper crustal melts (Holm et al., 2014) transported by the slab, as well as dehydration of serpentinites (Jacques et al., 2013). The limited range in isotopic values of Villarrica volcano that differ from most of the CHSEC data is indicative of a homogenous mantle source despite its substantially longer history of volcanic activity (~600 ky). Differences in magma sources of CHSEC and Villarrica volcano have also been suggested by Hickey-Vargas et al.

Table 4
Representative chemical analyses of minerals from CHSEC and the 1971 Villarrica eruption.

	Plagioclases				Olivines			
	HU-plph3	HU-plph5	SJ-plph3		VI-olph5	VI-olph4	HU-olph10	HU-olph9
SiO2	47.27	46.988	47.728	SiO2	38.864	38.664	38.794	39.526
Na2O	1.935	1.394	1.561	Al2O3	0.045	0.003	0.006	0.003
Al2O3	34.099	34.656	33.46	MgO	39.779	39.709	40.767	43.571
K2O	0.053	0.024	0.026	CaO	0.236	0.259	0.208	0.159
CaO	17.306	17.89	17.415	MnO	0.445	0.399	0.026	0.026
Total	100.663	100.952	100.190	FeO	21.175	21.892	20.835	17.897
XAn	90.51	77.258	92.418	Total	100.544	100.926	100.636	101.182
XAb	9.15	22.681	7.498	XFo	77	76	78	81
XOr	0.33	0.06	0.082	XFa	23	23	22	19

	Pyroxenes				Chromian-spinels		
	VI-pxph5	VI-pxph4	SJ-pxph3		CA-opin1	HU-opin1	VI-opin1
SiO2	51.774	52.154	52.526	Al2O3	27.616	26.98	12.319
Al2O3	2.791	2.666	2.917	MgO	12.833	12.11	7.882
MgO	16.804	16.877	16.962	CaO	0.007	0	0
CaO	18.42	19.562	22.641	TiO2	0.875	0.21	0.534
TiO2	0.574	0.574	0.3	Cr2O3	27.605	25.4	33.47
Cr2O3	0.452	0.452	0.381	FeO	12.02	35.28	12.83
MnO	0.275	0.204	0.15	Fe2O3	18.64	0	32.37
FeO	8.626	7.477	4.11	NiO	0.27	0.2	0.087
Fe2O3	0.076	0.15	0.961	Total	99.866	100.18	99.49
Total	99.792	100.142	100.948	#Mg	57.44	37.96	27.34
XEn	48.04	47.80	47.723	#Cr	33.4	38.71	61.66
XFs	11.94	12.13	6.494				
XWo	40.02	39.94	45.784				

For these and other clinopyroxenes and chromian-spinel inclusions the values of Cr-spinels Fe^{2+} and Fe^{3+} were obtained following Putirka's (2008) and Droop's (1987) propositions, respectively.

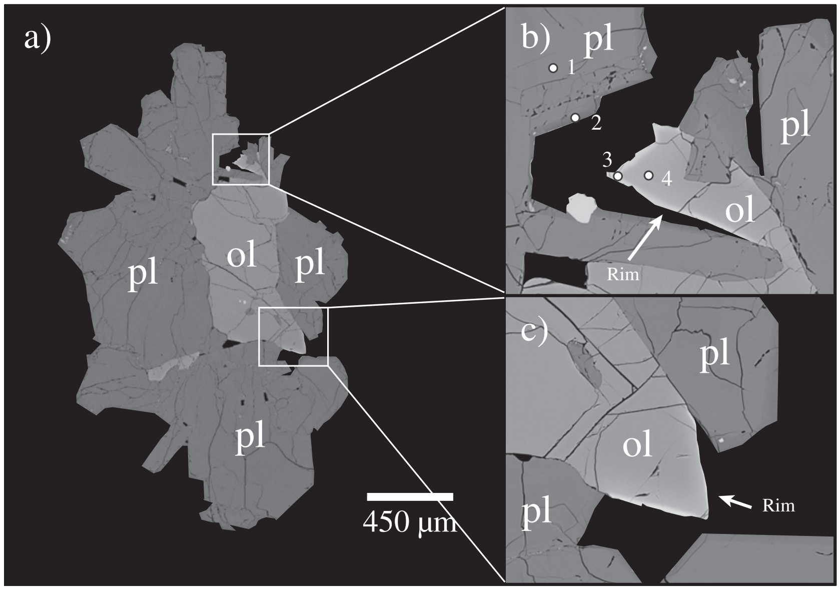

Fig. 10. a) Crystal clot of plagioclase and olivine phenocrysts from CHSEC (sample HUEL-1). b) and c) show details of olivine and plagioclase crystal exhibiting thin rims only in the non-armored crystal faces (i.e. in contact with the matrix). Numbered spots indicate the sites of EPM analyses. Analyses 1 (HU-plph3), 2 (HU-plph5), 3 (HU-olph10), and 4 (HU-olph9) are shown in Table 4.

(1989), however the cause of the observed isotopic similarities between Villarrica volcano and Cañi and San Jorge centers (Fig. 4) are still unknown.

5.2. Reservoirs at the mantle–crust boundary

5.2.1 . P,T conditions

The olivine–augite geothermometer (Loucks, 1996) and olivine–clinopyroxene geothermobarometer (Köhler and Brey, 1990) were used in the same olivine–clinopyroxene pairs (isolated phenocrysts or in crystal clots) of CHSEC and 1971 Villarrica lava (Table 3). The equilibrium conditions between olivine and augite pairs were tested using Grove et al. (1997) equations (Fig. 8) to determine if both minerals are in equilibrium with the same melt composition in terms of Fe/Mg values. Olivine–augite pairs of two CHSEC samples (CAB1-1 and SANJ-1) and two 1971 Villarrica lava samples (1971 10 M1 and 1971 N6) satisfied the mentioned equilibrium conditions with melts with Fe/Mg values of 0.5–0.6 (CHSEC) and 1–1.1 (Villarrica). These values are substantially different from those of the hosting sample composition, thus an antecrystic origin is inferred for these olivine and augite crystals. Equilibrium temperatures of ~1163 °C (1162–1165 °C ± 6 °C; Table 3; Fig. 8a) and pressures between 10.8 and 11.4 ± 1.7 kb (i.e. lower crust–upper mantle conditions) were obtained for the CHSEC olivine–augite antecryst pairs (Table 3). This wide pressure range includes the estimated pressure of ~10 kb (~35–40 km) for the mantle–crust boundary beneath the Andes at this latitude according to different techniques such as gravimetry (Folguera et al., 2007), earthquake traveltime tomography (Haberland et al., 2006), nearby receiver function profile (Dzierma et al., 2012a), and location of seismic clusters (Dzierma et al., 2012b). Although lower crust and upper mantle reservoirs cannot be ruled out, we favor a reservoir at the mantle–crust boundary because it constitutes a rheological barrier that facilitates mantle-derived magma storage (Hildreth and Moorbath, 1988). The absence in the CHSEC samples of thermobarometric evidence of shallow reservoirs or pauses during the magma ascent to the surface is consistent with a single-reservoir magma system. For the 1971 Villarrica lava temperatures of 1208 ± 6 °C (Fig. 8b) and pressure of 6.3–8.1 ± 1.7 kb were obtained from olivine–augite phenocrysts thermometry and barometry (Fig. 9c; Table 3). As with CHSEC, we favor the highest pressures for the Villarrica volcano deep reservoir (Fig. 10).

5.3. Shallow reservoir of the 1971 Villarrica lava

Conditions of a shallow magma reservoir for Villarrica volcano have been provided by Lohmar et al., (2012) from a study of the ~13 ky Licán Ignimbrite (pressures of <0.67 kb and T of ~900 and ~1100 °C as a consequence of heating). Shallow reservoir conditions of the 1971 Villarrica lava were also identified using the olivine–augite thermobarometry (sample 1971 10 M1): pressures up to 2.4 kb and associated temperatures of ~1170 °C (1164–1175 °C ± 6 °C; Table 3; Fig. 8) were calculated in olivine–augite pairs of a single clot (Fig. 9b; Table 4).

Additionally, the shallow reservoir conditions (P, T, f_{O2} and H_2O content) were calculated using MELTS (Ghiorso and Sack, 1995; Asimow and Ghiorso, 1998) by reproducing the compositions of Group 2 plagioclase cores ($An_{39–49}$) and plagioclase phenocryst rims (An_{74}). The Group 2 plagioclase core compositions were obtained under equilibrium at <0.8 kb, temperatures of 915–970 °C, dissolved H_2O content of 1–3.1 wt.% and NNO oxygen fugacities. Plagioclase rim compositions were also reproduced under equilibrium at similar pressures (<0.9 kb) and oxygen fugacities (NNO), but at higher temperatures (1120–1180 °C) and lower dissolved H_2O content (0.3–1.2 wt.%) than Group 2 plagioclase cores. By considering the plagioclase phenocryst rims as representative of the late stage of plagioclase formation at the shallow reservoir, these differences would indicate a heating and subsequent magma degassing prior to the eruption. Changes in pressure and water content associated with heating were also calculated by iteration of the empirical model equation for the solubility of water in basaltic melts (Moore et al., 1998) and the plagioclase-liquid hygrometer calibrated by Lange et al. (2009) (details in Appendix I). Using the same parameters (melt and plagioclase compositions), temperatures of 970 and 1180 °C were used for Group 2 plagioclase core compositions and plagioclase phenocryst rim compositions, respectively. The plagioclase anorthitic rim can only be reproduced as a consequence of temperature increase; it could not be reproduced using MELTS considering changes in P conditions and H_2O content.

The heating of the shallow reservoir at a calculated depth equivalent to 1.4–0.2 kb could be associated with H_2O exsolution of 1.7–0.2 wt.% (Fig. A1). We therefore speculate that heating by new hotter magma could generate volatile exsolution that triggered the 1971 eruption. A similar triggering mechanism has been invoked for the Licán Ignimbrite eruption in the Villarrica volcano, where the calculated time-scale for the reservoir temperature homogenization after the arrival of 200 °C hotter magma from below, is about few decades (Lohmar et al., 2012).

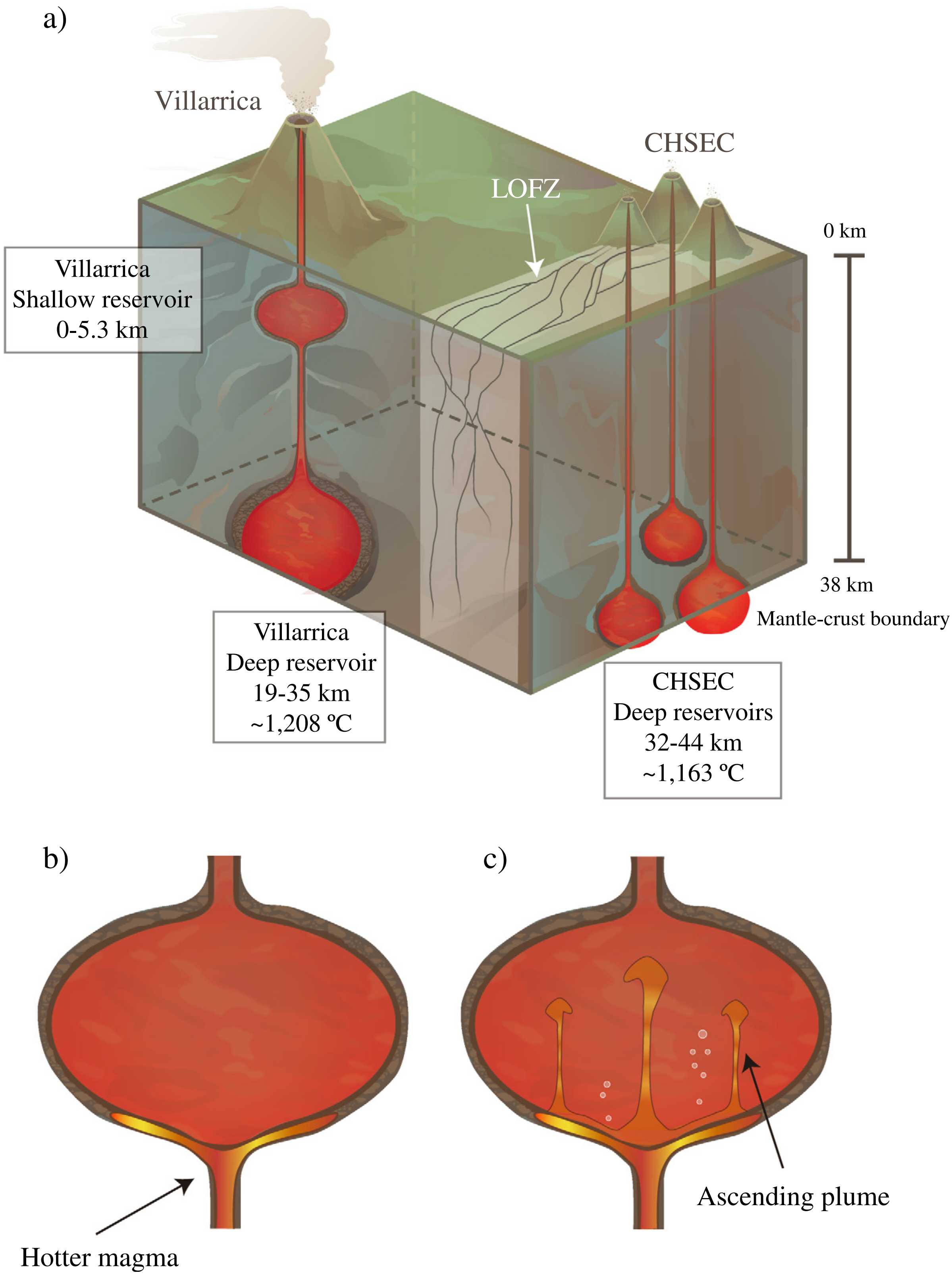

Fig. 11. a) Schematic representation of the main characteristics of the CHSEC and Villarrica reservoirs. Both studied volcanic complexes would have deep reservoirs at the mantle–crust boundary, but unlike the Villarrica volcano, CHSEC do not have a shallow reservoir probably by role of the LOFZ as an efficient conduit for the ascending magma. b) Villarrica volcano shallow reservoir during the arrival of hotter magma. c) Ascending plumes of heated magma in the shallow reservoir prior to eruption of 1971 lava.

5.4. Syn-eruptive conditions

We estimate syn-eruptive temperatures using equilibrium olivine–augite (Loucks, 1996) microlite pairs of four samples (Fig. 8) from both CHSEC (CAB1-1; CAB 1-2) and 1971 Villarrica lavas (1971 N6; 1971 10 M1). The calculated CHSEC temperature values are between 1081 and 1133 ± 6 °C (Fig. 8a), whereas olivine–augite microlite pairs of 1971 Villarrica lava gave values between 1123 and 1148 ± 6 °C (Fig. 8b).

Additionally, we reproduce by MELTS the temperature of the plagioclase microlite crystallization considering the microlite composition of the more abundant sizes: 30–60 μm (An_{59-60}) and 60–100 μm (An_{64-66}) for CHSEC and 1971 Villarrica lava, respectively. The calculated CHSEC syn-eruptive temperatures are between 1130 and 1137 °C at crystal content between 45 and 52 vol.%. For the 1971 Villarrica eruption the calculated temperatures are between 1150 and 1160 °C at crystal content between 23 and 35 vol.%. It is interesting to note that the 1971Villarrica lava plagioclase microlites crystallized at slightly lower temperatures than those of plagioclase phenocryst rims (1180 °C) but higher than the 970 °C of the Group 2 plagioclase core crystallization, consistent with the mentioned heating as a triggering mechanism of the eruption.

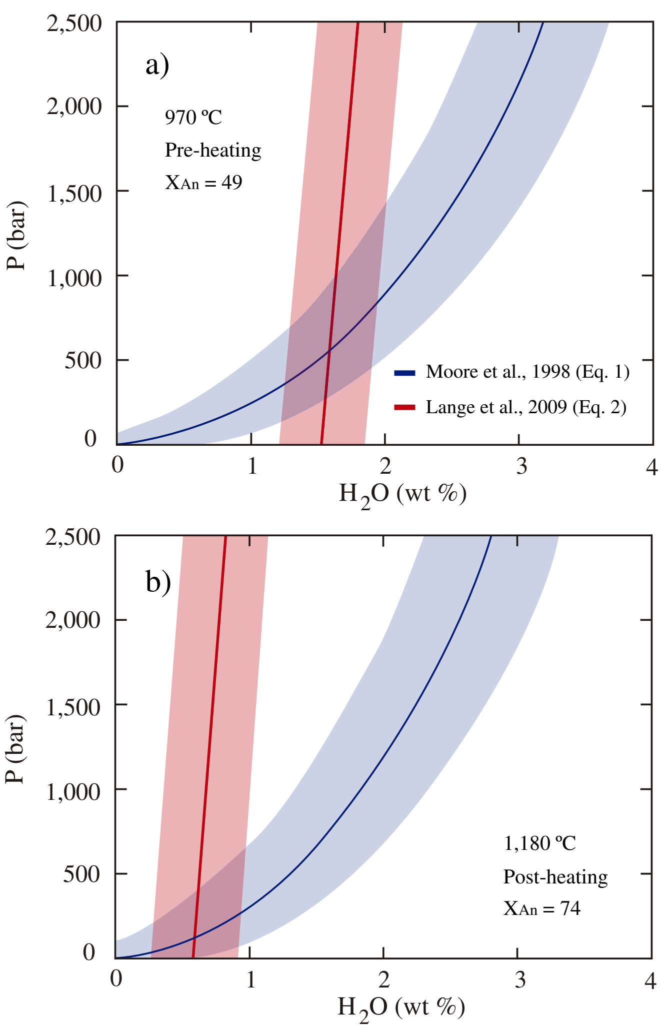

Fig. A1. Numerical solution to determine variations of pressure conditions and H_2O concentration of the shallow reservoir associated with heating. A maximum pressure of 1.4 kb for the shallow reservoir and an exsolution between 1.2 and 0.2 wt.% after 210 °C heating were calculated. Decompression of up to 1.4 kb was calculated for this heating event. Red lines represent Lange's et al. (2009) equation and blue lines represent Moore's et al. (1998) equation. The uncertainties of each equation (Moore's et al., 1998 and Lange's et al., 2009) are shown as corresponding fields.

Despite the high crystallinity calculated for the selected CHSEC lava, the effective consistencies determined from the modified Einstein-Roscoe equation (Castruccio et al., 2010) are between 4 and 16 kPa s, which are adequate for a basaltic lava to flow (e.g. 1984 Mauna Loa eruption; Lipman and Banks, 1987).

6. Conclusions

The Caburgua-Huelemolle Small Eruptive Centers (CHSEC) and Villarrica Volcano are an example of coexistence of small eruptive centers and stratovolcanoes, a feature very common in the Southern Volcanic Zone. There are similarities between the CHSEC and 1971 Villarrica lavas. In both cases the lavas were fed from deep reservoirs with temperature and pressure conditions coincident with the depth of mantle–crust boundary. However, there are significant differences with respect to pre-eruptive upper crustal magma history. CHSEC magmas would have migrated directly to the surface from the deep reservoir, whereas the 1971 Villarrica lava would have had a more complex history consistent with higher rates of magma supply (relative low rates would be associated with monogenetic volcanism; Takada, 1994) and with an intermediate reservoir at shallow depth that underwent a heating episode prior to eruption Fig. 11.

The active LOFZ that controls the distribution of CHSEC could facilitate a direct transport to the surface of their magmas ponded at the base of the crust, whereas the Villarrica Volcano is built over an inactive NW–SE basement fault (Moreno and Clavero, 2006). This tectonic situation, together with the overburden exerted by the Villarrica Volcano edifice, would have hindered the magma ascent (see Pinel and Jaupart, 2000) and facilitated the shallow reservoir construction.

Acknowledgments

We acknowledge Chris L. Hayward, for his help with the microprobe at School of Geosciences, University of Edinburgh. Alina Guereschi, Gustavo Castellano and Fernando Colombo, provided us assistance with the microprobe at LAMARX—National University of Córdoba. Fruitful discussion with Nicolas Vinet, Diego Aravena, and Ignacio Villalón at the University of Chile, are greatly appreciated. The financial support through FONDAP project 15090013 MSc fellowships (EM and CC) and CONICYT MSc fellowship (22130368, CC) is acknowledged. Anonymous reviewers provided valuable comments and suggestions that substantially improved this manuscript.

Appendix I

We calculated the magma H_2O solubility and pressure conditions of the 1971 Villarrica shallow reservoir from a melt composition equivalent to the R1971 DV sample (Table 2) through an iterative combination of the following expressions provided by Moore's et al. (1998) and Lange et al. (2009):

Moore's et al. (1998) expression:

$$2ln^{melt}X_{H_2O} = \frac{a}{T} + \sum b_i X_i \frac{P}{T} + c\, ln^{fluid} f_{H_2O} + d \quad (A1)$$

where ${}^{melt}X_{H_2O}$ is the mole fraction of H_2O dissolved in the melt, T is temperature (Kelvin), P is pressure (bar), X_i is the anhydrous mole fraction of melt components, and a, b, c and d are the regression coefficients.

Lange's et al., (2009) expression:

$$^{melt}X_{H_2O} = m'x + a' + \frac{b'}{T} + \sum d_i' X_i \quad (A2)$$

where x is a variable state dependent on enthalpy, entropy, volume, pressure, temperature and melt and crystallizing plagioclases compositions; m', a', b' and d'_i are regression coefficients of calibration.

This approach assumes core/rim Group 2 plagioclase phenocrysts composition (An_{49}/An_{74}) and temperatures of crystallization of 970/1180 °C (respectively). A temperature increase of ~200 °C was recognized as the trigger of the eruption of the 13 ky Licán Ignimbrite (Lohmar et al., 2012). The resulting pressures were between 1.4 and 0.15 kb previous to this heating event (for core plagioclases crystallization), whereas after heating the pressure was up to 0.67 kb (for rim plagioclases crystallization). The calculated H_2O content of the melt prior to heating is between 2 and 1.2 wt.% (for plagioclase core crystallization), whereas after the heating is between 1 and 0.3% (for plagioclase rim crystallization). Therefore, the heating is associated with water exsolution (from 0.2 to 1.7 wt.%) and could be related to a decompression of up to 1.4 kb (equivalent to ~5.3 km), probably as a consequence of the ascent of magma or the opening of the magmatic system at the beginning of the eruption.

Appendix II. Supplementary data

Supplementary data to this article can be found online at http://dx.doi.org/10.1016/j.jvolgeores.2015.09.023.

References

Aravena, D., Lahsen, A., 2012. Assessment of exploitable geothermal resources using magmatic heat transfer method, Maule Region, Southern Volcanic Zone, Chile. Geotherm. Res. Counc. Trans. 36, 1307–1313.

Asimow, P.D., Ghiorso, M.S., 1998. Algorithmic modifications extending melts to calculate subsolidus phase relations. Am. Mineral. 83, 1127–1131.

Brand, B.D., White, C.M., 2007. Origin and stratigraphy of phreatomagmatic deposits at the Pleitocene Sinker Butte Volcano, Western Snake River Plain, Idaho. J. Volcanol. Geotherm. Res. 160, 319–339. http://dx.doi.org/10.1016/j.jvolgeores.2006.10.007.

Brenna, M., Cronin, S.J., Smith, I.E., Maas, R., Sohn, Y.K., 2012. How small-volume basaltic magmatic systems develop: a case study from the Jeju Island volcanic field, Korea. J. Petrol. 53 (5), 985–1018. http://dx.doi.org/10.1093/petrology/egs007.

Calder, E., Harris, A., Peña, P., Pilger, E., Flynn, L., Fuentealba, G., Moreno, H., 2004. Combined thermal and seismic analysis of the Villarrica Volcano lava lake, Chile. Rev. Geol. Chile 31 (2), 259–272. http://dx.doi.org/10.4067/S0716-02082004000200005.

Cañón-Tapia, E., Walker, G.P.L., 2004. Global aspects of volcanism: the perspective of "plate tectonics" and "volcanic systems. Earth Sci. Rev. 66, 163–182. http://dx.doi.org/10.1016/j.earscirev.2003.11.001.

Castruccio, A., Rust, A.C., Sparks, R.S.J., 2010. Rheology and flow of crystal-bearing lavas: insights from analogue gravity currents. Earth Planet. Sci. Lett. 297, 471–480. http://dx.doi.org/10.1016/j.epsl.2010.06.051.

Cembrano, J., Lara, L., 2009. The link between volcanism and tectonics in the southern volcanic zone of the Chilean Andes: a review. Tectonophysics 471, 96–113. http://dx.doi.org/10.1016/j.tecto.2009.02.038.

Cembrano, J., Hervé, F., Lavenu, A., 1996. The Liquiñe Ofqui fault zone: a long lived intra-arc fault system in southern Chile. Tectonophysics 256, 55–66. http://dx.doi.org/10.1016/0040-1951(95)00066-6.

Clavero, J., Moreno, H., 1994. Ignimbritas Licán y Pucón: evidencias de erupciones explosivas andesítico–basálticas postglaciales del Volcán Villarrica, Andes del Sur, 39°25′S. 7th Congreso Geológico Chileno, Concepción, Chilepp. 250–254.

Clavero, J., Moreno, H., 2004. Evolution of Villarrica Volcano. In: Lara, L., Clavero, J. (Eds.), Villarrica Volcano (39.5°S), Southern Andes, Chile. Boletín 61. Servicio Nacional de Geología y Minería, Santiago, pp. 17–27.

Condit, C.D., Connor, C.B., 1996. Recurrence rates of volcanism in basaltic volcanic fields: an example from the Springerville volcanic field, Arizona. Geol. Soc. Am. Bull. 108, 1225–1241. http://dx.doi.org/10.1130/0016-7606(1996)108<1225:RROVIB>2.3.CO;2.

Connor, C.B., Condit, C.D., Crumpler, L.S., Aubele, J.C., 1992. Evidence of regional structural controls on vent distribution — Springerville Volcanic Field, Arizona. J. Geophys. Res. 97, 12349–12359. http://dx.doi.org/10.1029/92JB00092.

Connor, C.B., Stamatakos, J.A., Ferrill, D.A., Hill, B.E., Ofoegbu, G.I., Conway, F.M., Sagar, B., Trapp, J., 2000. Geologic factors controlling patterns of small-volume basaltic volcanism: application to a volcanic hazards assessment at Yuca Mountain, Nevada. J. Geophys. Res. 105 (1), 417–432. http://dx.doi.org/10.1029/1999JB90035.

Conway, F.M., Connor, C.B., Hill, B.E., Conduit, C.D., Mullaney, K., Hall, C.M., 1998. Recurrence rates of basaltic volcanism in SP Cluster, San Francisco volcanic field, Arizona. Geology 26 (7), 655–658. http://dx.doi.org/10.1130/0091-7613(1998)026<0655:RROBVI>2.3.CO.

Davidson, J., Turner, S., Plank, T., 2013. Dy/Dy*: variations arising from mantle sources and petrogenetic processes. J. Petrol. 54 (3), 525–537. http://dx.doi.org/10.1093/petrology/egs076.

Droop, G.T.R., 1987. A general equation for estimating Fe^{3+} concentrations in ferromagnesian silicates and oxides from microprobe analyses, using stoichiometric criteria. Mineral. Mag. 51, 431–435. http://dx.doi.org/10.1180/minmag.1987.051.361.10.

Dzierma, Y., Thorwart, M., Rabbel, W., 2012a. Moho topography and subducting oceanic slab of the Chilean continental margin in the maximum slip segment of the 1960 Mw 9.5 Valdivia (Chile) earthquake from P-receiver functions. Tectonophysics 530-531, 180–192. http://dx.doi.org/10.1016/j.tecto.2011.12.016.

Dzierma, Y., Thorwart, M., Rabbel, W., Siegmund, C., Comte, D., Bataille, K., Iglesia, P., Prezzi, C., 2012b. Seismicity near the slip maximum of the 1960 Mw 9.5 Valdivia earthquake (Chile): plate interface lock and reactivation of the subducted Valdivia Fracture Zone. J. Geophys. Res. 117, B06312. http://dx.doi.org/10.1029/2011JB008914.

Folguera, A., Introcaso, A., Giménez, M., Ruiz, F., Martínez, P., Tunstall, C., García Morabito, E., Ramos, V., 2007. Crustal attenuation in the Southern Andean retroarc (38°–39°30′ S) determined from tectonic and gravimetric studies: the Lonco-Luán asthenospheric anomaly. Tectonophysics 439, 129–147. http://dx.doi.org/10.1016/j.tecto.2007.04.001.

Ghiorso, M.S., Sack, R.O., 1995. Chemical mass transfer in magmatic processes: IV. A revised and internally consistent thermodynamic model for the interpolation and extrapolation of liquid–solid equilibria in magmatic systems at elevated temperatures and pressures. Contrib. Mineral. Petrol. 119, 197–212. http://dx.doi.org/10.1007/BF00307281.

Grove, T.L., Donnelly-Nolan, J.M., Housh, T., 1997. Magmatic processes that generated the rhyolite of Glass Mountain, Medicine Lake Volcano, N. California. Contrib. Mineral. Petrol. 127, 205–223. http://dx.doi.org/10.1007/s004100050276.

Gutiérrez, F., Gioncada, A., González-Ferrán, O., Lahsen, A., Mazzuoli, R., 2005. The Hudson Volcano and surrounding monogenetic centres (Chilean Patagonia): an example of volcanism associated with ridge–trench collision environment. J. Volcanol. Geotherm. Res. 145 (3–4), 207–233.

Haberland, C., Rietbrock, A., Lange, D., Bataille, K., Hofmann, S., 2006. Interaction between forearc and oceanic plate at the south-central Chilean margin as seen in local seismic data. Geophys. Res. Lett. 33, L23302. http://dx.doi.org/10.1029/2006GL028189.

Hickey-Vargas, R., Moreno, H., López Escobar, L., Frey, F., 1989. Geochemical variations in Andean basaltic and silicic lavas from the Villarrica–Lanín volcanic chain (39.5°S): an evaluation of source heterogeneity, fractional crystallization and crustal assimilation. Contrib. Mineral. Petrol. 103, 361–386. http://dx.doi.org/10.1007/BF00402922.

Hickey-Vargas, R., Sun, M., López-Escobar, L., Moreno, H., Reagan, M.K., Morris, J.D., Ryan, J.G., 2002. Multiple subduction components in the mantle wedge: evidence from eruptive centers in the Central Southern volcanic zone, Chile. Geology 30, 199–202. http://dx.doi.org/10.1130/0091-7613(2002)030<0199:MSCITM>2.0.CO;2.

Hildreth, W., Moorbath, S., 1988. Crustal contributions to arc magmatism in the Andes of Central Chile. Contrib. Mineral. Petrol. 98 (4), 455–489. http://dx.doi.org/10.1007/BF00372365.

Holm, P.M., Søager, N., Dyhr, C.T., Nielsen, M.R., 2014. Enrichments of the mantle sources beneath the Southern Volcanic Zone (Andes) by fluids and melts derived from abraded upper continental crust. Contrib. Mineral. Petrol. 167. http://dx.doi.org/10.1007/s00410-014-1004-8.

Houghton, B.F., Schmincke, H.U., 1989. Rothenberg scoria cone, East Eifel: a complex strombolian and phreatomagmatic volcano. Bull. Volcanol. 52, 28–48. http://dx.doi.org/10.1007/BF00641385.

Irvine, T.N., Baragar, W.R.A., 1971. A guide to the chemical classification of the common volcanic rocks. Can. J. Earth Sci. 8 (5), 523–548. http://dx.doi.org/10.1139/e71-055.

Jacques, G., Hoernle, K., Gill, J., Hauff, F., Wehrmann, H., Garbe-Schönberg, D., van den Bogaard, P., Bindeman, I., Lara, L.E., 2013. Across-arc geochemical variations in the Southern Volcanic Zone, Chile (34.5–38.0°S): constraints on mantle wedge and slab input compositions. Geochim. Cosmochim. Acta 123, 218–243. http://dx.doi.org/10.1016/j.gca.2013.05.016.

Kay, S.M., Godoy, E., Kurtz, A., 2005. Episodic arc migration, crustal thickening, subduction erosion, and magmatism in the south-central Andes. Geol. Soc. Am. Bull. 117, 67–88. http://dx.doi.org/10.1130/B25431.1.

Köhler, T.P., Brey, G.P., 1990. Calcium exchange between olivine and clinopyroxene calibrated as a geothermobarometer for natural peridotites from 2 to 60 kb with applications. Geochim. Cosmochim. Acta 54, 2375–2388. http://dx.doi.org/10.1016/0016-7037(90)90226-B.

Lange, R.A., Frey, H.M., Hector, J., 2009. A thermodynamic model for the plagioclase-liquid hygrometer/thermometer. Am. Mineral. 94, 494–506. http://dx.doi.org/10.2138/am.2009.3011.

Lara, L., Lavenu, A., Cembrano, J., Rodríguez, C., 2006a. Structural controls of volcanism in transversal chains: resheared faults and neotectonics in the Cordón Caulle–Puyehue area (40.5°S), Southern Andes. J. Volcanol. Geotherm. Res. 158, 70–86. http://dx.doi.org/10.1016/j.jvolgeores.2006.04.017.

Lara, L., Moreno, H., Naranjo, J.A., Matthews, S., Pérez de Arce, C., 2006b. Magmatic evolution of the Puyehue–Cordón Caulle Volcanic Complex (40° S), Southern Andean Volcanic Zone: from shield to unusual rhyolitic fissure volcanism. J. Volcanol. Geotherm. Res. 157, 343–366. http://dx.doi.org/10.1016/j.jvolgeores.2006.04.010.

Le Bas, M.J., Le Maitre, R.W., Streckeisen, A., Zanettin, B., 1986. A chemical classification of volcanic-rocks based on the total alkali silica diagram. J. Petrol. 3, 745–750. http://dx.doi.org/10.1093/petrology/27.3.745.

Lewis-Kenedi, C.B., Lange, R.A., Hall, C.M., Delgado-Granado, H., 2005. The eruptive history of the Tequila volcanic field, western Mexico: ages, volumes, and relative proportions of lava types. Bull. Volcanol. 67, 319–414. http://dx.doi.org/10.1007/s00445-004-0377-3.

Lipman, P.W., Banks, N.G., 1987. Aa flow dynamics, Mauna Loa. In: Decker, W., Wright, T.L., Stauffer, P.H. (Eds.), Volcanism in Hawaii. US Geological Survey Professional Paper 1350, pp. 1527–1567.

Lohmar, S., Robin, C., Gourgaud, A., Clavero, J., Parada, M.A., Moreno, H., Ersoy, O., López-Escobar, L., Naranjo, J.A., 2007. Evidence of magma–water interaction during the 13,800 years BP explosive cycle of the Licán Ignimbrite, Villarrica Volcano (Southern Chile). Rev. Geol. Chile 34 (2), 233–247.

Lohmar, S., Parada, M.A., Gutiérrez, F., Robin, C., Gerbe, M.C., 2012. Mineralogical and numerical approaches to establish the pre-eruptive conditions of the mafic Licán Ignimbrite, Villarrica Volcano (Chilean Southern Andes). J. Volcanol. Geotherm. Res. 235 – 236, 55–69. http://dx.doi.org/10.1016/j.jvolgeores.2012.05.006.

López-Escobar, L., Cembrano, J., Moreno, H., 1995a. Geochemistry and tectonics of the Chilean Southern Andes basaltic quaternary volcanism (37–46°S). Rev. Geol. Chile 22 (2), 219–234.

López-Escobar, L., Parada, M.A., Hickey-Vargas, R., Frey, F.A., Kempton, P.D., Moreno, H., 1995b. Calbuco Volcano and minor eruptive centers distributed along the Liquiñe-Ofqui Fault Zone, Chile (41° – 42° S): contrasting origin of andesitic and basaltic magma in the Southern Volcanic Zone of the Andes. Contrib. Mineral. Petrol. 119, 345–365. http://dx.doi.org/10.1007/BF00286934.

Loucks, R., 1996. A precise olivine–augite Mg–Fe-exchange geothermomete. Contrib. Mineral. Petrol. 125, 140–150. http://dx.doi.org/10.1007/s004100050211.

McGee, L.E., Beier, C., Smith, I.E.M., Turner, S., 2011. Dynamics of melting beneath a small-scale basaltic system: a U–Th–Ra study from Rangitoto Volcano, Auckland volcanic field, New Zealand. Contrib. Mineral. Petrol. 162 (3), 547–563. http://dx.doi.org/10.1007/s00410-011-0611-x.

Moore, G., Vennemann, T., Carmichael, I.S.E., 1998. An empirical model for the solubility of H_2O in magmas to 3 kilobars. Am. Mineral. 83, 36–42.

Moreno, H., 1993. Volcán Villarrica. Geología y evaluación del riesgo volcánico, regiones IX y X, 39°25′S. Servicio Nacional de Geología y Minería.

Moreno, H., Clavero, J., 2006. Geología del volcán Villarrica, Regiones de La Araucanía y de Los Lagos. Servicio Nacional de Geología y Minería, Carta Geológica de Chile, Serie Geología Básica, No. 98, Mapa escala 1:50000.

Moreno, H., Lara, L., 2008. Geología del área Pucón-Curarrehue, regiones de La Araucania y De Los Ríos. Servicio Nacional de Geología y Minería, Carta Geológica de Chile, Serie Geológica Básica. No. 115, Mapa Escala 1:100.000.

Németh, K., 2010. Monogenetic volcanic fields: origin, sedimentary record, and relationship with polygenetic volcanism. In: Cañón-Tapia, E., Szakács, A. (Eds.), What is a volcano?: Geological Society of America Special Paper 470, pp. 43–66.

Park, J.B., Park, K.H., Cho, D.L., Koh, G.W., 1999. Petrochemical classification of the Quaternary volcanic rocks in Cheju Island, Korea. J. Geol. Soc. Korea 35, 253–264.

Pinel, V., Jaupart, C., 2000. The effect of edifice load on magma ascent beneath a volcano. In: Francis, P., Neuberg, J., Sparks, R.S. (Eds.), The Causes and Consequences of Eruptions of Andesite Volcanoes; Papers of a Discussion Meeting. Philosophical Transactions — Royal Society. Mathematical, Physical and Engineering Sciences 358, pp. 1515–1532.

Pinel, V., Jaupart, C., 2004. Magma storage and horizontal dyke injection beneath a volcanic edifice. Earth Planet. Sci. Lett. 221, 245–262. http://dx.doi.org/10.1016/S0012-821X(04)00076-7.

Putirka, K.D., 2008. Thermometers and barometers for volcanic systems. Rev. Mineral. Geochem. 69, 61–120.

Silva, C., Druitt, T., Robin, C., Lohmar, S., Clavero, J., Moreno, H., Naranjo, J.A., 2004. The 3700-yr Pucón eruption of Villarrica Volcano, 39°S Southern Andes, Chile. International Association of Volcanology and Chemistry of the Earth's Interior (IAVCEI) General Assembly, Pucón, Chile.

Stern, C., 1991. Role of subduction erosion in the generation of Andean magmas. Geology 19, 78–81. http://dx.doi.org/10.1130/0091-7613.

Stern, C., 2011. Subduction erosion: rates, mechanisms, and its role in arc magmatism and the evolution of the continental crust and mantle. Gondwana Res. 20, 284–308. http://dx.doi.org/10.1016/j.gr.2011.03.006.

Stern, C.R., Moreno, H., López-Escobar, L., Clavero, J.E., Lara, L.E., Naranjo, J.A., Parada, M.A., Skewes, M.A., 2007. Chilean volcanoes. In: Moreno, T., Gibbons, W. (Eds.), The Geology of Chile. The Geological Society, London, pp. 147–178.

Sun, S., McDonough, W.F., 1989. Chemical and isotopic systematics of oceanic basalts; implications for mantle composition and processes. In: Saunders, A.D., Norry, J.M. (Eds.), Magmatism in the Ocean Basins, Special Publications. Geological Society of London 42, pp. 313–345.

Takada, A., 1994. Accumulation of magma in space and time by crack interaction. In: Ryan, M.P. (Ed.), Magmatic Systems. Academic Press, San Diego, California.

Valentine, G.A., Gregg, T.K.P., 2008. Continental basaltic volcanoes — processes and problems. J. Volcanol. Geotherm. Res. 177, 857–873. http://dx.doi.org/10.1016/j.jvolgeores.2008.01.050.

Valentine, G.A., Perry, F.V., 2006. Decreasing magmatic footprints of individual volcanoes in a waning basaltic field. Geophys. Res. Lett. 33. http://dx.doi.org/10.1029/2006GL026743.